ECTI Transactions on Computer and Information Technology
Journal homepage: https://ph01.tci-thaijo.org/index.php/ecticit/
Published by the ECTI Association, Thailand, ISSN: 2286-9131

UAV-Based mmWave MIMO with PSO-Enhanced Hybrid OMA-NOMA Access

Ameer Y. Sadeeq[1] and Mohamad A. Ahmed[2]

ABSTRACT

This paper presents a UAV-based communication system that integrates hybrid Orthogonal Multiple Access (OMA) and Non-Orthogonal Multiple Access (NOMA) schemes, operating in the millimeter-wave (mm-Wave) frequency band and supported by Multiple-Input Multiple-Output (MIMO) technology. The proposed Hybrid OMA/NOMA-mm-Wave MIMO framework is designed to enhance overall system performance by delivering high-capacity wireless connectivity to ground users (GUs). UAVs act as aerial base stations (BSs), offering rapid and flexible communication services in diverse real-world scenarios, including natural disasters, areas lacking fixed infrastructure, and temporary coverage at large public events. To improve NOMA's performance, a Particle Swarm Optimization (PSO) algorithm is employed for optimizing power allocation (PA), ensuring fairness between near and far users. Furthermore, a user pairing mechanism integrated with optimized power allocation is introduced to enhance the UAV-BS performance in mm-Wave-NOMA scenarios. The channel model considers both line-of-sight (LoS) and non-line-of-sight (NLoS) conditions, incorporating angle of departure (AoD), angle of arrival (AoA), and Doppler effects. Simulation results demonstrate that NOMA outperforms OMA in specific scenarios, while OMA remains more effective in others. PSO-based power allocation significantly surpasses fixed PA schemes in NOMA systems.

Article information:

Keywords: Non-orthogonal Multiple Access (NOMA), Particle Swarm Optimization (PSO), Pairing Algorithms (PA), Successive Interference Cancellation (SIC), Unmanned Aerial Vehicle (UAV)

Article history:
Received: August 7, 2025
Revised: October 9, 2025
Accepted: October 16, 2025
Published: October 25, 2025 (Online)

DOI: 10.37936/ecti-cit.2025194.263116

1. INTRODUCTION

ntegrating non-orthogonal multiple access (NOMA) with millimetre (mm-Wave) and multiple-input-multiple-output (MIMO) of unmanned aerial vehicles (UAVs), locally known as the drone, has been a great interest in the world of wireless communications systems recently, as shown in Fig. 1,which shows UAV-BS at a certain altitude providing service to some users on the ground using NOMA technology with millimeter-wave (mm-wave) frequencies, to support many applications beyond fifth-generation (B5G) wireless networks. The mentioned system provides huge bandwidth with a high data rate, due to its high frequencies [1], [2]. NOMA technology provides the users with service simultaneously in non-orthogonal resources separated between users by power level. In contrast, the conventional orthogonal multiple access (OMA) technology provides the users service orthogonal resources without depending on various power level users such as time-division multiple access (TDMA)[3].

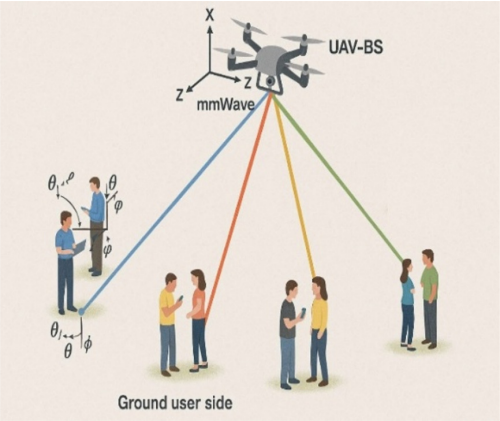

Fig. 1: *Unmanned Aerial Vehicle Base Station (UAV-BS) Network Model.*

[1,2]The authors are with the College of Electronics Engineering, Ninevah University, Mosul, Iraq, Email: ameer.yaseen@stu.uoninevah.edu.iq and mohamad.alhabbar@uoninevah.edu.iq
[1]Corresponding author: ameer.yaseen@stu.uoninevah.edu.iq

In contrast, communication over mm-wave is a strong candidate to be employed in B5G and 6G networks. This technique available a large bandwidth which supports high throughput and low latency for UAV-BS communication systems, in such systems, the UAV-BS is fixed on flying in space while grounding users (GU) are distributed on the ground, this assumption is valid when the infrastructure of fixed BS is not available as in the remote areas, and it is required to provide telecommunication services for users in this area. The frequency range of mm-wave communication is from 30 to 300 GHz, which is considered one of the uncongested spectrums in that a large bandwidth can be obtained, which consequently leads to enhancing the overall system's capacity[4]. The comparisons between OMA and NOMA-based UAVs over sub-6GHz are presented in [5], in which the outage probability and the sum rates for the two techniques are investigated.

The line-of-sight (LOS) link between UAV-BS and ground users is fully suitable for mm-Wave communication to obtain high beamforming gain, and the non-line-of-sight (NLOS) link between UAV-BS and ground users is often heavily attenuated [6]-[7].

To further enhance the spectral efficiency (SE) of the system, mm-wave-based MIMO techniques have been employed in the NOMA UAV-BS [8]. Furthermore, the short wavelength of mm-wave technology enables the installation of a large number of antennas in a small physical area, which is beneficial for UAV-BS applications [9], where the typical wavelength of mm-wave signal is between 1 mm to 10 mm. For instance, at 38 GHz, the half-wavelength spacing between array antenna elements enables the integration of over 600 antennas within a 1 square decimeter (10 cm^2) area. Such compact components are particularly advantageous for weight and size-constrained platforms like drones. Conversely, mm-wave is highly vulnerable to obstacles due to the significant penetration and reflection characteristics of millimeter signals. During signal radiation from a UAV-BS to ground users, any motion of either the UAV-BS or the ground user induces the Doppler effect. This, in turn, causes carrier frequency offset (CFO) and inter-carrier interference (ICI). Due to the high carrier frequency and high mobility, Significant Doppler shifts are especially pronounced in mmWave UAV communication systems [10].

It is noteworthy that the endurance of untethered multirotor UAVs indeed depends on the type of energy source and payload configuration. According to [20], the typical flight duration of electric multirotor UAVs with realistic communication payloads ranges between 20 and 40 minutes, while hybrid-electric or fuel-cell platforms can provide extended operation. However, the consideration of UAV fuel type, power source, and energy management systems lies outside the scope of this paper, which primarily focuses on the communication performance modeling. Therefore, stationary and tethered UAV scenarios are beyond the intended analytical framework of this work [20].

1.1 Main Contributions and Literature Overview

In this study, the investigation emphasizes hybrid orthogonal multiple access (OMA) and non-orthogonal multiple access (NOMA) aid millimeter-wave (mm-Wave) with multiple-input multiple-output (MIMO) technology across unfixed base stations via UAVs.

- Multiple users have been considered during this study to be served over the mm-Wave channels, in which a determination of the channel capacity is obtained over different types of channels, i.e., LoS and NLoS between UAV-BS and the ground user. Moreover, the determination and analysis of several performance metrics, including outage probability, sum rate, and bit error rate (BER), are obtained. Furthermore, the impact of the distance on data rate, outage probability, and BER are taken into account. For more precise channel modeling, both elevation and azimuth components are included in modeling the angle of arrival (AoA) and angle of departure (AoD), while the link conditions account for potential obstructions such as buildings, located in urban areas, or free space, is taken into account to determine the appropriate path loss exponent.
- A pairing algorithm is used to improve spectral efficiency, which consequently enhances the performance of the overall system. This operation is achieved by grouping UAV-BS users based on channel gains, data rate requirements, and distance. After that, pair each strong user with the weak user as one group.
- The millimeter-wave (mmWave) frequency band has been considered in the design of UAV-based base station (UAV-BS) based OMA-NOMA hybrid systems to significantly enhance data rate performance. By leveraging the wide bandwidth available in the mm-wave spectrum, the system can support higher transmission rates, reduced latency, and improved spectral efficiency, making it a promising solution for next-generation wireless communication networks.
- The Doppler effect has been considered in this research paper, in which any inconsistency between the UAV-BS and the ground user perhaps affects the channel linking between them. We assume a Doppler frequency of 300Hz and provide an estimate of this effect on system performance over the NOMA and OMA mechanisms.
- Power optimization plays an important role in this research, as it directly affects the overall performance of the UAV-BS over the mm-Wave OMA-NOMA hybrid system. Two techniques have been

implemented to explain this parameter: a fixed Power Allocation Factor (PAF) approach, where predefined values are assigned to users manually, and a Particle Swarm Optimization (PSO)-based PAF method, which automatically searches by special algorithm for the optimal power distribution to maximize system performance metrics mentioned earlier.

- Compared to[9], which made a comparison between the NOMA and OMA over fixed mm-Wave MIMO setups, i.e., lacking UAV mobility and Doppler considerations, this work proposes significant extension by analyzing a mobile UAV-BS system with user pairing, dynamic channel conditions, and power optimization throughout applying PSO, offering a more realistic and complex scenario.
- While [10] focused on Doppler effects under full UAV mobility, it focused only on channel behavior and did not explore power optimization or multiple access techniques. Our study includes Doppler but expands beyond to system-level metrics like BER and outage over NOMA/OMA and balances communication system performance analysis with practical implementation techniques like PSO-based power allocation and user pairing.
- The authors in[11] offer a survey on a broad and insightful overview of power-domain NOMA systems in the context of emerging technologies such as mm-Wave, MIMO, and fixed UAVs, while the mobility of the UAV in the presence of Doppler effects is the main contribution discussed and analyzed in this work.

2. SYSTEM MODEL

We assume UAV-BS is equipped with mm-Wave NOMA MIMO as shown in Fig. 1. The moving BS by UAV provides the service for several GUs defined as $\{GU_1, GU_2, GU_3 \ldots\ldots GU_N\}$. These ground users are distributed in a specific area of land. The grounding users are divided into groups, in which two users are paired in one group by applying a pairing algorithm. The ground users (GUs) are positioned at varying distances from the UAV-BS, denoted as $\{\mathrm{d}_{GU_1}, \mathrm{d}_{GU_2}, \mathrm{d}_{GU_3}, \ldots\ldots \mathrm{d}_{GU_N}\}$.

Multiple scenarios are considered to evaluate the achievable rates of the ground users (GUs), the UAV-BS's sum rate, the error probability, i.e. the bit error rate (BER), and the spectral efficiency (SE) for the proposed system via applying orthogonal multiple access (OMA) and NOMA through the mmWave channel while accounting for Doppler effects and his effect on our results. Furthermore, testing the different distances on the outage probability and data rate for users.

Utilizing the NOMA technique, the highest amount of power allocation coefficient is assigned to weak channel condition channels, and the lowest power allocation coefficient is assigned to strong channel gain [12]. We assume the UAV-BS provides service for four GUs, the first user GU_1 is considered the nearest one from UAV-BS, the second GU is further away than the first, the third GU is further away than the first and the second GU and the fourth is the farthest one from UAV-BS, i.e.$\{\mathrm{d}_{GU_4} > \mathrm{d}_{GU_3} > \mathrm{d}_{GU_2} > \mathrm{d}_{GU_1}\}$. The power allocation factors (PAFs) are denoted by $a_1, a_2, a_3, \ldots, a_N$ for those users. According to GUs' distances, PAF for GUs will be chosen as $a_4 > a_3 > a_2 > a_1$ in this scenario.

In addition, successive interference cancellation (SIC) is required to be employed for all users' receivers except the user who has the largest PAF, i.e., the user with a weak channel condition, at this user the interference caused by other users can be represented by additive noise.

At first GU, the achievable rate is evaluated as[12] :

$$R_1 = B \log_2 \left(1 + \frac{a_1 p\_t g_1}{n_1}\right) \tag{1}$$

where p_t is the total transmit power by UAV-BS to all GUs, the PAF, the noise power, and the channel gain for the k^{th} user is denoted by a_k, n_k, and g_k, respectively. It can be seen that (1) has included the signal-to-noise ratio (SNR) rather than the SINR due to applying SIC at this user who has allocated the smallest portion of power.

The second ground user (GU2) is located farther from the UAV-BS than GU1, but the fourth GU (GU4) is the farthest overall, requires a higher power allocation factor (PAF) due to its weaker channel gain (i.e., i.e.,$(a_2 > a_1)$.Successive Interference Cancellation (SIC) must be applied by all users except the farthest one to remove the superposed signals of users with stronger channels, as previously discussed.

Therefore, the achievable rate at GU_2 after removing the signal of GU_3 and GU_4 by SIC is given as

$$R_2 = B \log_2 \left(1 + \frac{a_2 p\_t g_2}{a_1 p\_t g_2 + n_2}\right) \tag{2}$$

While the third GU needs to assign more power than GU_1 and GU_2 due to poor channel gain, i.e. $(a_3 > a_2 > a_1)$, the achievable rate at U_3 is computed as:

$$R_3 = B \log_2 \left(1 + \frac{a_3 p\_t g_3}{a_1 p\_t g_3 + a_2 p\_t g_3 + n_3}\right) \tag{3}$$

GU_4, being the farthest user from the UAV-BS, is allocated the largest portion of power to compensate for its weak channel conditions. The power allocation factors a_1, a_2, a_3 corresponding to the nearer users are treated as interference. Accordingly, the achievable rate for GU4 is calculated as:

$$R_4 = B\log_2\left(1+\frac{a_4 p\_tg_4}{a_1 p\_tg_4 + a_2 p\_tg_4 + a_3 p\_tg_4 + n_4}\right) \quad (4)$$

On the other hand, assuming the OMA technique is employed instead of NOMA to provide the service for the same four users, the computation of achievable rates for any user follows the method in [13]:

$$R_k^{OMA} = 0.5B\log_2\left(1+\frac{p\_tg_k}{n_k}\right) \quad (5)$$

For the k^{th} user in the NOMA system, the average individual achievable rate can be expressed as:

$$\bar{R}_k = E\{R_k\}, \quad (6)$$

where $E\{\cdot\}$ denotes the expectation operator. Similarly, the average individual achievable rate for any user served by OMA is given by:

$$\bar{R}_k^{OMA} = E\{R_k^{OMA}\} \quad (7)$$

The sum rate (SR) of the NOMA system, i.e. the total rate provided by the UAV-BS, can be computed by adding the individual rates of all users.

$$SR_{NOMA} = \sum_{n=1}^{N} R_n \quad (8)$$

The sum rate of the OMA system is obtained by summing the individual rates of all users.

$$SR_{OMA} = \sum_{n=1}^{N} R_n^{OMA} \quad (9)$$

Furthermore, the spectral efficiency (SE), in bits/sec/Hz (bps/Hz), for NOMA or OMA can be evaluated as [12]:

$$SE = \frac{SR}{BW} \quad (10)$$

3. STATUS LINK BETWEEN UAV-BS AND GU

In any wireless communication system, the channel link represents the connection between the transmitting station (UAV-BS) and the receiving station (GU). The quality of this channel is heavily influenced by the line-of-sight (LoS) or non-line-of-sight (NLoS) conditions.

The received power by k^{th} user computed as follows [13]:

$$Prx_k(dB) = Ptx(dB) - L_k(dB) \quad (11)$$

Here, Ptx represents the transmission power of the UAV-BS, and L_k denotes the path loss of the air-to-ground (A2G) channel between the UAV-BS and the k^{th} ground user (GU). The path loss L_k over the distance X_k is calculated following the method described in [14], accounting for both line-of-sight (LoS) and non-line-of-sight (NLoS) conditions, as given by:

$$L_k = 10\eta\log_{10}(X_k) + X_{LoS}, \quad (12)$$

$$L_k = 10\eta\log_{10}(X_k) + X_{NLoS}. \quad (13)$$

The parameter η, known as the path-loss exponent, plays a crucial role in wireless communication modeling. Its magnitude is determined by environmental factors including interference, reflection, and diffraction effects.

Additionally, the LoS probability between a ground user and the UAV-BS is characterized by the expression provided in[13]:

$$Pr_{LoS}(k) = \frac{1}{1+\alpha\exp(-\beta[\theta_k - \alpha])} \quad (14)$$

Here, α and β are environment-dependent constants that vary based on the type of area, e.g., urbanurban ($\alpha = 0.3$, $\beta = 500$), dense urban ($\alpha = 0.5$, $\beta = 300$).cIn this context, $\alpha\backslash\alpha\alpha$ denotes the proportion of ground surface covered by buildings relative to the total area (dimensionless), β reflects the density of buildings in the area and is measured in terms of the number of buildings per square kilometer (buildings/km^2).

The probability of a non-line-of-sight (NLoS) link between UAV-BS and GU is given as [13]:

$$Prj(NLoS) = 1 - Prj(LoS) \quad (15)$$

Generally, the UAV does not have information about the terrain type in its flight zone, making it difficult to determine whether the link is LoS or NLoS. Therefore, equation (11) can be reformulated as follows[13]

$$Prx, j(dB) = Ptx(dB) - \bar{L}_j(Rc, H) \quad (16)$$

where $\bar{L}_j(Rc, H)$ the expression represents the mean path loss, incorporating the probabilityof both line-of-sight (LoS) and non-line-of-sight (NLoS) scenarios connections between the GU and UAV-BS, and is determined by the following equation [13]

$$\bar{L}_k(Rc, H) = Prk(LoS)L_k(LoS) + Prk(NLoS)L_k(NLoS) \quad (17)$$

To determine the distance between the UAV-BS and the ground user, we represent the 2D coordinates of the UAV-BS as (X_{UAV}, Y_{UAV}) and the 2D location of the ground user as (X_{GU}, Y_{GU})The distance between UAV-BS and GU is expressed as[14]

$$d_g = \sqrt{(X_{UAV} - X_{GU})^2 + (Y_{UAV} - Y_{GU})^2 + H^2} \quad (18)$$

where H represents to altitude of UAV-BS, the chan-

nel h between the UAV-BS and GU (also called the Saleh-Valenzuela channel) is determined by[15]:

$$h = \sqrt{\frac{G_a N_r N_t}{\beta_{GU-UAV} P_{GU-UAV}}} \sum_{p=1} c_i e^{j2\pi f_D t} a_r\left(\phi^p_{GU-UAV}\right) a_t^H\left(\psi^p_{GU-UAV}\right) \tag{19}$$

where G_a is the antenna gain, N_r and N_t number of receive and transmit respectively. Also, the P_{GU-UAV} represents to number of propagation paths, e.g., LoS and NLoS multipaths, between GU and UAV-BS. Furthermore,

C_i is the tap's amplitude where represents to is the complex amplitude (gain and phase) of the i^{th} multipath component, i.e., represents the attenuation and initial phase of the path. Moreover, a_r and a_t represent the normalized receive and transmit array response vectors at a UAV-BS and a GU, respectively, where ϕ^p_{GU-UAV} represents the angle of arrival (AoA) at the UAV-BS for the p-th path and ψ^p_{GU-UAV} represents the the angle of departure (AoD) from the UAV-BS for the p-th path , while $e^{j2\pi f_D t}$ represents the Doppler-induced phase shift due to relative motion between the transmitter and receiver, where f_D is the Doppler shift frequency (in Hz) which is defined as:

$$f_D = \frac{u}{C}\cos\theta \tag{20}$$

where u is the relative speed between the transmitter and receiver typically the UAV's speed (in meters/second), while C is the speed of light, and θ represents the angle between the direction of motion of the UAV (or user) and the direction of the incoming signal (LoS path).

Furthermore, $a_r(\cdot)$ and $a_t(\cdot)$ represent normalized receive and transmit array response vectors respectively [16], where $a_r(\phi_{GU-UA})$ expressed by:

$$a_r(\phi_{GU-UAV}) = \frac{1}{\sqrt{Nr}}\left[e^{j\frac{2\pi d}{\lambda} n \sin(\phi_{GU-UAV})}\right]_{n=0}^{N_r-1} \tag{21}$$

and $a_r(\phi_{GU-UAV})$ expressed by:

$$a_t(\phi_{GU-UAV}) = \frac{1}{\sqrt{Nt}}\left[e^{j\frac{2\pi d}{\lambda} n \sin(\phi_{GU-UAV})}\right]_{n=0}^{N_t-1} \tag{22}$$

It is worth mentioning that λ and d represent the wavelength and the spacing between antenna elements, also, ϕ_{GU-UAV} and ψ_{GU-UAV} refer to the angle of arrival (AoA) and angle of departure (AoD) of p^{th} path. In addition, n and m indices over receive/transmit antenna elements, moreover, β_{GU-UAV} denotes the path loss (in dB) between UAV-BS and GU is expressed as follows

$$\beta_{GU-UAV} = B_0 + 10\eta\log_{10}\left(\frac{d_{GU-UAV}}{d_0}\right) + A\zeta \tag{23}$$

$$B_0 = 10\log_{10}\left(\frac{4\pi d_0}{\lambda}\right)^2 \tag{24}$$

Here, $d_0 = 1m$ is the reference distance. In addition, d_{GU-UAV} represent the distance between UAV-BS and GU, $A\zeta$ represents a zero-mean Gaussian random variable with a standard deviation ζ (in dB), modeling the effect of shadow fading. The parameter η denotes the path loss exponent, which varies based on environmental conditions such as interference, terrain, and obstacle density.reflections, and diffraction [17]In this paper, we assume the UAV-BS link with the GU is obstructed by buildings, representing a typical urban environment. A path-loss exponent of 4 to 6 is used to model the increased attenuation due to NLOS conditions. Furthermore, we consider the path-loss exponent for the LoS case equal to 2.

4. POWER OPTIMIZATION

It is the key aspect of UAV-BS, especially when serving several GUs under the MIMO-NOMA framework in the mm-wave technology. As previously mentioned, the power level in NOMA varies from one GU to another according to some factors related to GU based on user channel conditions to achieve the required performance.

In other words, balancing the PAF between near and far user power levels directly impacts the sum rate and outage probability.

In this study, two different approaches are employed to allocate the PAF for NOMA users: manual selection and automatic optimization by the Particle Swarm Optimization (PSO) algorithm. The first method involves assigning fixed power values to users based on predefined criteria or assumptions. While this approach offers simplicity and ease of implementation, however, it struggles to adapt to changing channels and user needs.

The second method is automated optimization of the power by using the PSO algorithm to determine the optimal power allocation dynamically. Furthermore, power levels are based on real-time parameters such as channel gain, user distance, and data rate demands. As a result, the automatic power allocation method is much better than the first method for achieving the high data rate user with lower outage probability.

PSO algorithm begins determining the NOMA of all users' channels by setting the transmitter power by UAV-BS for each user and finding the noise power and the interference level. However, assigning the swarm size (number of particles in the swarm) and assigning the long search number of the swarm (Maximum

number of iterations) is the second step. The PSO first randomly generates large values of PAF starting from 0.01 to 0.99 for the user with the weakest channel condition, and depending on this random PAF, it allocates PAFs for other users with less portion of power. Following, compute the fitness for each particle based on the total sum rate. PSO algorithm.

By keeping the local best and the global best for each particle result can be obtained from the swarm through the iterations process. Consequently, we use inertia to update the velocity of a particle with update the position and assign new PAF according to the new position within [0.01, 0.99] to improve the NOMA sum rate. Continuously update until the best position for particle which gives the optimal power allocation between far and near users. The PSO algorithm is shown in Table1.

Table 1: *Particle Swarm Optimization PSO algorithm.*

1: Input: h_2 far user, total transmit power Pt, noise power σ^2, swarm size N, maximum iterations T, Doppler f_D, UAV speed V_{UAV}, carrier frequency fc, distances far user, angles (AOD, AOA) at far user, PSO parameters (W, C1, C2, rand ()), Antenna gain Ga, Number of propagation paths P_{GU-UAV} , light speed C, Complex amplitude (gain and phase) of the i^{th} multipath component C_i , Doppler angle θ, transmitter and receiver array factor (at and ar), Path loss between UAV and use LU−UAV, MIMO Antennas M × N
2: Initialize particle positions: αi ∈ [0.01, 0.99] randomly for i = 1 to N (αi = NOMA PA ratio for far user).
3: Initialize velocities $v_i = 0$ for all particles.
4: For each particle i = 1 to N:
Compute fitness: f_i = -sum_rate (α_i, h_1, h_2, P_t, σ^2)
5: Set personal bests:
p_best$_i$ = α_i, f_best$_i$ = f_i
6: Set global best:
g_best = α_i with best (lowest) f_best$_i$
7: For t = 1 to T do:
8: For i = 1 to N do:
9: Update channel gain far user:
h_2 = generate Channel (d2, Pt, σ^2, f_D, V_{UAV}, fc, θ_{fD}, AOD, AOA, Ga,P_{GU-UAV} , C, C_i , at, ar, LU−UAV, M × N)
10: Update velocity:
$v_i = w \cdot v_i + c_1 \cdot rand() \cdot (p\_best_i - \alpha_i) + c_2 \cdot rand() (g\_best - \alpha_i)$
11: Update position: $\alpha_i = \alpha_i + v_i$
12: Clamp α_i within [0.01, 0.99]
13: Compute new fitness:
f_i = -sum_rate (α_i, h_2, P_t, σ^2)
14: Update personal best: If fi < f_besti:
p_besti = αi, f_besti = fi
Else: keep p_besti and f_besti unchanged
15: Update g_best among all p_best$_i$
Output: Optimal NOMA PA α = g_best
(FU gets α·P_t, NU gets (1–α) ·P_t)

5. PAIRING USERS

Use pairing in NOMA technology to enhance the spectral efficiency and achieve the demand user data rate with increased fairness power distribution between Near-far users thus improving NOMA performance compared to OMA. Initially, the algorithm evaluates the channel quality of every user covered by the UAV-BS. In simpler terms, the user suffering from low channel gain will get high power i.e. far user (FU), whereas the user with good channel gain will get low power i.e. near user (NU) [18].In the paper, we assume multiple users under the coverage area of UAV-BS are divided into groups i.e.

clusters, each two pairing users is considered as one group K to serve $2K$ users. The pairing algorithm arranges the user channel gain in descending order to to allocate transmission power levels among users in the coverage area i.e., $g_1 \geq g_(2) \geq \ldots\ldots\ldots g_2M$. The first group was created by UAV-BS by pairing the nearest user characterized by the highest channel gain, g_1, with the user having the lowest channel gain, g_{2K} (farthest user). Afterwards paring the second user having channel gain, g_2, with users g_{2K-1}. The mentioned operation will be finished until all users are in their clusters. This method of paring called near-far pairing (N-F). Table 2 illustrates the near-far pairing algorithm for NOMA users [5].

Table 2: *Algorithm for Pairing NOMA NU and FU [19].*

1: Input: Start with the channel gains for all users, represented as a vector $g_n = [g_1, g_2, \ldots\ldots g_{2K}]$, number of user pairs K, number of users, $2K$.
2: Classifying: Arrange the channel gains in descending order so that: $g_1 \geq g_2 \geq \ldots\ldots\ldots g_{2M}$.
3: Initialization: Define a set Q containing all sorted channel gains, i.e., $Q = \{g_1, g_2, \ldots\ldots g_{2K}\}$
4: Pairing Process:
For each pairing, index $i = 1$ *to* K

Identify the **strongest** and **weakest** users from the current set Q:

$$g_{max} = max\ (Q)$$
$$g_{min} = min\ (Q)$$

Form a user pair as: $g_n = \{g_{max}, g_{min}\}$
Update the set Q by removing the selected maximum and minimum gains.

5: Result: The result is a set of K user pairs, each comprising one strong and one weak user based on their respective channel gains.

6. RECEIVER DETECTION PROCEDURE

Each user (far and near users) within the group will receive the superimposed NOMA signal from UAV-BS, the superimposed includes the signal of the near user which has a strong channel gain with a signal of the far user which has a poor channel gain. As mentioned above, a low power allocation factor (PAF) is assigned to the near user (NU) with strong channel

gain, while a higher PAF is allocated to users experiencing weaker channel gain. The high PAF of the far user will influence on near user as interference. To remove this effect, the SIC operation will apply near near-user detection signal of FU with high PAF which is subsequently subtracted from the superimposed NOMA signal to retrieve the signal from NU free of interference. By comparison, unlike the NU, the FU's signal is detected directly without SIC, considering the NU's interference, with a low power allocation factor, as additive noise. The receiver detection procedure is explained in Fig.2.

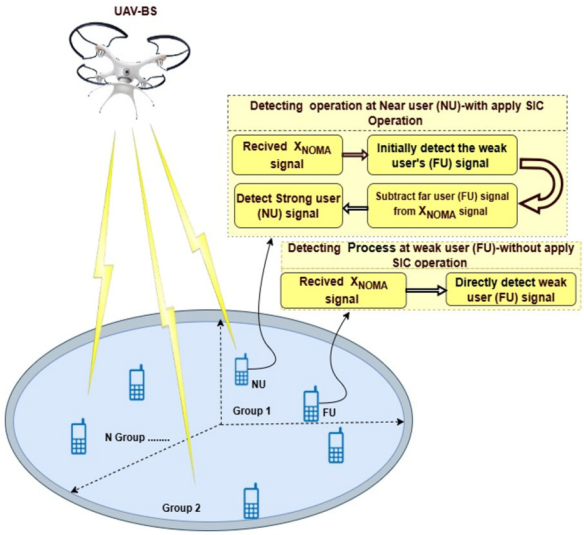

Fig.2: *Detection process of the NOMA signal at the receivers of the near and far users post-pairing.*

7. RESULTS AND DISCUSSION

For the evaluation of performance metrics including bit error rate, Pout, and the sum rate, the effects of distances and motions of UAV and user are considered. As well known that any motion leads to the Doppler effect which may cause different performance results. A performance comparison between the proposed NOMA-based system and the traditional OMA approach is conducted across multiple scenarios over an mm-wave communication channel. As previously stated, the UAV-BS delivers wireless services to several users.

This study assumes that two users, specifically, the near user (NU) and the far user (FU), are grouped into one cluster by implementing a pairing algorithm. This pairing strategy is designed to exploit the differences in channel conditions between users, allowing for the implementation of the NOMA technique to enhance the throughput and spectrum efficiency. As a result, the overall performance of the network is improved in terms of both spectral efficiency and service quality for users with varying channel characteristics with use BPSK modulation.

Table 3: *Outlines the parameters employed in the simulation.*

Notation	Description	Value
η_{L_0S}	Path loss exponent	2
η_{NL_0S}	Path loss exponent	4
d_{FU}	Link distance between UAV-BS and FU	130m
d_{NU}	Link distance between UAV-BS and NU	90m
a_F^{manual}	Power allocation coefficient for Far User (manual)	0.7
a_N^{manual}	Power allocation coefficient for Near User (manual)	0.3
a_F^{PSO}	Power allocation for Far User (optimized by PSO)	0.01 – 0.99
a_N^{PSO}	Power allocation for Near User (optimized by PSO)	$1 - a_F^{PSO}$
$N_t \times N_t$	MIMO antenna configuration	{8×2}
p_t	Transmit power by UAV-BS	0 to 40 dBm
R_F	Desired throughput for the FU	3 bps/Hz
R_N	Desired throughput for the NU	5 bps/Hz
f_o	Operating frequency	28 GHz
BW	Bandwidth	850 MHz
f_D	Doppler _ Frequency	300 Hz
V_{UAV}	Velocity of UAV-BS	10 m/s
d_λ	Antenna spacing	0.5 λ
$(\boldsymbol{\phi}\ \&\ \boldsymbol{\theta})_{UAV}$	Azimuth & Elevation angles for Far and near-user (UAV-BS)	$\{30^0, 45^0\}$ and $\{90^0, 45^0\}$
$(\boldsymbol{\phi}\ \&\ \boldsymbol{\theta})_{GUs}$	Azimuth & Elevation angles for Far and near-user (GUs)	$\{60^0, 30^0\}$ and $\{60^0, 30^0\}$

The first case study explores the deployment of a MIMO-NOMA system, where the UAV-BS is equipped with N_t antennas, serving users equipped with N_r antennas each. The path-loss model considers two scenarios to represent varying propagation conditions. In the free space, i.e., the LoS case is the dominant, where there are no obstructions, the path-loss exponent is set to 2. In contrast, obstruction caused by buildings is modeled as a suburban environment, where partial or complete blockage increases attenuation.

As aforementioned, two distinct methods are used to determine the PAF for NOMA users: a manual assignment approach which uses 0.3 and 0.7 for near-far users respectively. The second method uses an automated optimization technique based on the PSO algorithm. In this study, both manual and PSO-based methods are used for power allocation in NOMA systems. The manual method assigns fixed PAF values, while the PSO algorithm automatically optimizes them. A performance comparison is conducted to evaluate the effectiveness of each approach.The

channel bandwidth of 850MHz is employed throughout the analysis. Furthermore, the Angles of Departure (AoD) at the UAV-BS are assumed to be $\{60°, 45°\}$ for the Far User (FU) and $\{45°, 30°\}$ for the Near User (NU), representing the azimuth and elevation angles, respectively. On the Ground User (GU) side, the Angles of Arrival (AoA) are considered as $\{60°, 30°\}$ for the FU and $\{30°, 30°\}$ for the NU. It is noteworthy that Table 3 includes all the parameters that were assumed in our simulation to obtain the results and comparisons.

Figure 3 illustrates the sum rate performance of NOMA and OMA for the proposed system under identical conditions, comparing two power allocation factor (PAF) strategies: fixed PAF and PSO-optimized PAF. The first technique applies a fixed power allocation factor (PAF), where 70% of the total power is assigned to the far user and 30% to the near user. The second technique employs the PSO algorithm to adaptively determine the optimal PAF for the far user within the range of 0.01 to 0.99, while the near user receives the remaining portion.

As seen in the plot, the NOMA scheme with PSO-optimized PAF consistently achieves the highest sum rate across the entire range of transmit powers (0–40 dBm). This demonstrates the significant advantage of adaptive power allocation via PSO in efficiently managing user interference and improving spectral efficiency in NOMA systems.

In contrast, both OMA configurations (with fixed and PSO PAF) exhibit lower sum rates, indicating the inherent limitations of orthogonal transmission in utilizing available resources. Although PSO optimization slightly enhances OMA performance compared to fixed PAF, the improvement is modest.

NOMA with fixed PAF outperforms OMA, but remains inferior to PSO-optimized NOMA, emphasizing the value of dynamic power allocation.

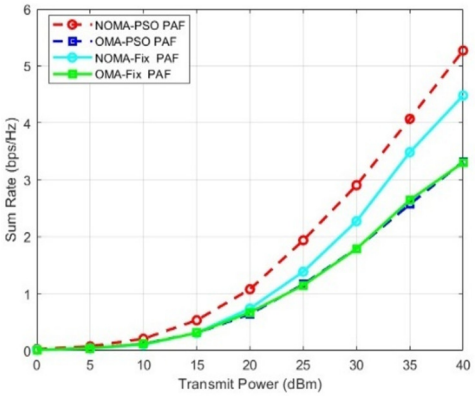

Fig.3: *Effect of different PAF methods on NOMA and OMA sum rate performance.*

Fig. 4 illustrates the individual data rates of the FU and the NU evaluated under MIMO-NOMA and MIMO-OMA schemes, implemented by the UAV-based base station (UAV-BS), under two power allocation factor (PAF) techniques: fixed PAF and fixed PAF with PSO. For the NU, NOMA with PSO provides the highest data rate by efficiently allocating minimal power to the far user, benefiting the NU's strong channel. However, for the FU, NOMA with fixed PAF yields better performance than PSO, as fixed allocation reserves more consistent power for the far user, while PSO may favor the near user to maximize the sum rate. In contrast, OMA limits both users due to time/frequency splitting. NU in OMA achieves slightly higher rates due to better channel conditions. However, far users suffer significantly from reduced power.

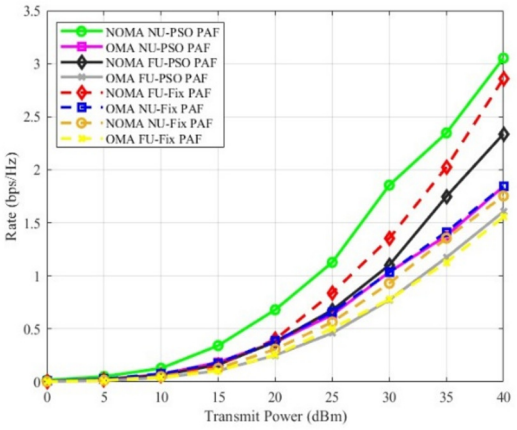

Fig.4: *Individual data rates of NU and FU using NOMA and OMA with fixed and PSO-based power allocation.*

At a transmit power of 35 dBm, as observed from Fig. 5 that the far user (FU) in the NOMA scheme under the fixed PAF achieves the lowest outage probability among all scenarios. This outcome can be attributed to the high-power allocation favoring the far user in the fixed strategy, which enhances signal strength and reliability at the cell edge. Additionally, the NU and FU in the NOMA scheme with PSO-PAF exhibit a reasonably low outage probability, indicating that the adaptive optimization effectively balances power between users to maintain acceptable performance for both NU and FU.

The Doppler impact on the sum rate performance of NOMA and OMA systems under both fixed and PSO-optimized PAFs is illustrated in Fig.6, showing that as the Doppler frequency increases from 0 Hz to 200 Hz, the sum rate decreases significantly for all schemes due to increased channel variation, with NOMA consistently outperforming OMA in both fixed and optimized scenarios and the PSO-based PAF approach providing superior performance over fixed PAF in both NOMA and OMA configurations.

In Fig.7 the achievable data rate versus transmit power for four GUs (GU1–GU4) located at increas-

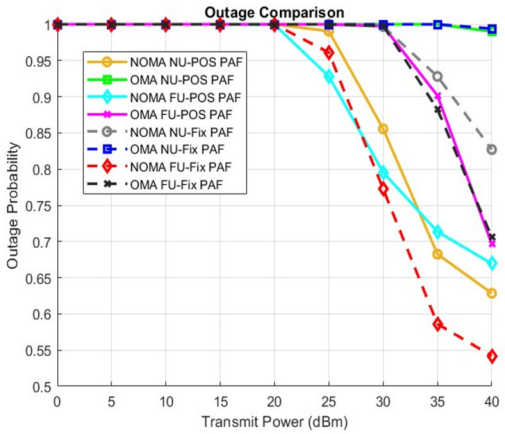

Fig.5: *The outage probabilities of the FU and NU under NOMA and OMA schemes under two different PAF techniques.*

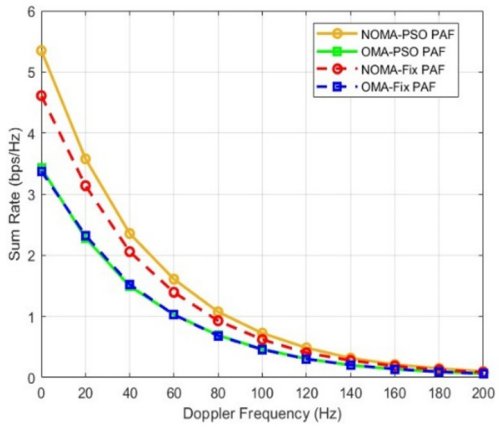

Fig.6: *Effect of Doppler Frequency on NOMA and OMA Sum Rate Performance.*

ing distances from a UAV-BS: 90m, 120m, 150m, and 200m. Two power allocation strategies are compared: PSO-based PAF optimization and fixed PAF. When the transmit power is increased, the data rate improves for all users. However, an increase in the user's distance from the UAV-BS drives decreases in achievable rate, attributed to higher path loss in mm-wave communication. NUs (e.g., U1 at 90m) are characterized by higher data rates compared to FUs (e.g., U4 at 200m). Generally, the fixed PAF outperforms PSO for FUs.

Fig.8 shows the outage probability performance for four users located at different distances (90m, 120m, 150m, and 200m) under two power allocation strategies. When the user distance increases, the outage probability also increases for both techniques due to higher path loss and reduced signal strength and that leads to an increased BER at the user. It is interesting to note that PSO-based PAF is created to adaptively optimize PAF, the Fixed PAF approach explains superior performance in reducing outage probability over all distances and transmit power levels.

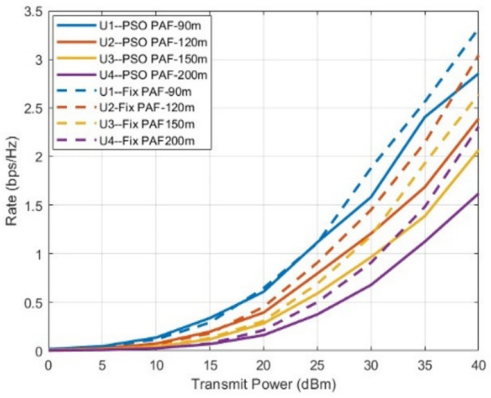

Fig.7: *Impact of user distance on data rate.*

The performance gap after 30 dBm is more noticeable at higher transmit powers, where Fixed PAF keeps lower outage probabilities compared to the PSO-PAF.

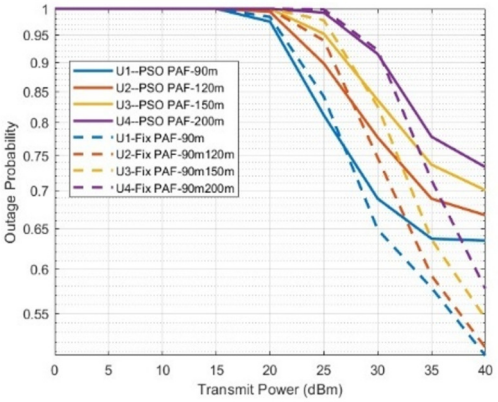

Fig.8: *Outage probability performance for users located at different distances.*

The relationship between the BER and data rate (ranging from 0.5 to 3.5 bps/Hz) for both NU and FU NOMA and OMA schemes is represented in Fig. 9, it can be noticed that the BER decreases for all schemes when the data rate increases. Due to good channel gain with high PAF, the NU NOMA and OMA achievable low BER compare with FU due to having poor channel gain. To summarize, NOMA-UN outperformed OMA-NU.

In the last fig.10. relation to the outage probability with a range of data rates from (0.5 to 3.5) bps/Hz for both NU and FU under NOMA and OMA schemes. As the data rate increases, the outage probability decreases for all users. Generally, for both users the NOMA superiority OMA, that is belong to allows multiple users to share the same resources by allocating different power levels according to channel user status, giving high power to FU and less power to NU.

In the last Fig.11, the Energy Efficiency (EE) performance of a NOMA system under two power allocation strategies: PSO-based dynamic alloca-

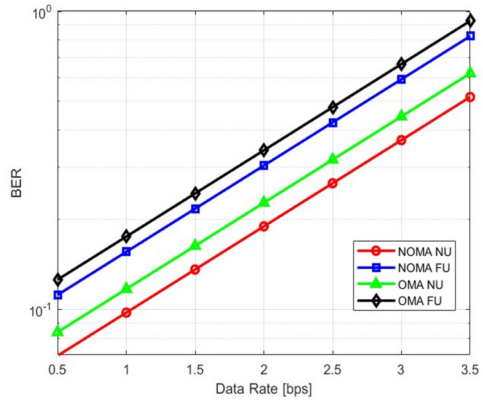

Fig.9: *Bit error rate (BER) for NOMA -OMA users at different data rates.*

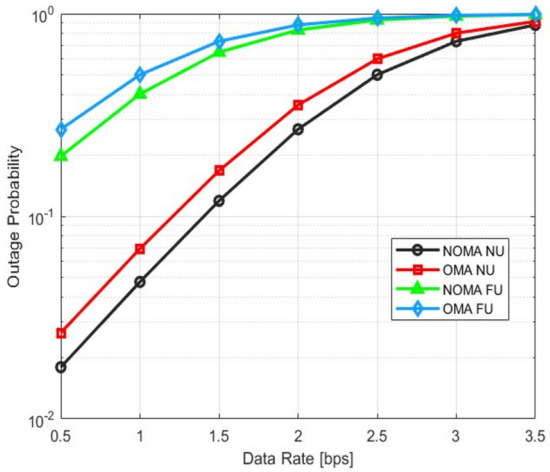

Fig.10: *Outage probability for NOMA -OMA users at different data rates.*

tion and fixed power allocation factor (PAF). The PSO approach achieves significantly higher EE across all transmit power levels, peaking at around 1.75 bps/Hz/W at 25 dBm. In contrast, the fixed PAF method shows lower efficiency, indicating suboptimal power usage. The results demonstrate the advantage of using optimization algorithms like PSO for enhancing energy efficiency in NOMA systems.

8. CONCLUSIONS

A UAV-based base station featuring multiple antennas and mm-Wave operation is introduced to provide connectivity to multiple ground users using a hybrid OMA–NOMA scheme. A near–far user pairing strategy was applied, where OMA was used between clusters and NOMA within clusters. To enhance system fairness and spectral efficiency, a Particle Swarm Optimization (PSO) algorithm was employed for adaptive power allocation. Comprehensive simulations were conducted under varying channel conditions, including LoS and NLoS scenarios, accounting for AoD, AoA, and Doppler effects due to

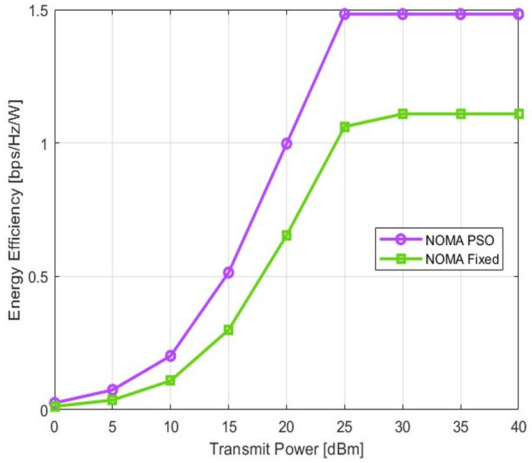

Fig.11: *Energy Efficiency Comparison of NOMA Schemes with PSO and Fixed Power Allocation.*

UAV mobility. The results demonstrated that NOMA offers significant performance gains over OMA in clustered environments, particularly when coupled with adaptive power allocation via PSO. These findings confirm the potential of hybrid OMA–NOMA systems for UAV-assisted communication, especially in dynamic or emergency scenarios. Future work could explore the integration of Intelligent Reflecting Surfaces (IRS) to improve signal strength in NLoS conditions and the development of dynamic access-switching mechanisms to ensure uninterrupted service.

AUTHOR CONTRIBUTIONS

Conceptualization, Ameer Yaseen and Mohamad Ahmed; methodology, Ameer Yaseen; software, Ameer Yaseen; validation, Ameer Yaseen and Mohamad Ahmed; formal analysis, Ameer Yaseen; investigation, Ameer Yaseen; data curation, Ameer Yaseen; writing—original draft preparation, Ameer Yaseen; writing—review and editing, Ameer Yaseen and Mohamad Ahmed; visualization, Ameer Yaseen; supervision, Mohamad Ahmed; funding acquisition, Mohamad Ahmed.

References

[1] N. Rupasinghe, Y. Yapici and I. Guevenc, "Performance of Limited Feedback Based NOMA Transmission in mmWave Drone Networks," *2018 IEEE International Conference on Communications Workshops (ICC Workshops)*, Kansas City, MO, USA, pp. 1-6, 2018.

[2] W. Belaoura, K. Ghanem, M. Z. Shakir and M. O. Hasna, "Performance and User Association Optimization for UAV Relay-Assisted mm-Wave Massive MIMO Systems," in *IEEE Access*, vol. 10, pp. 49611-49624, 2022.

[3] N. Rupasinghe, Y. Yapici, I. Güvenç and Y.

Kakishima, "Non-orthogonal multiple access for mmWave drones with multi-antenna transmission," *2017 51st Asilomar Conference on Signals, Systems, and Computers*, Pacific Grove, CA, USA, pp. 958-963, 2017.

[4] Y. Tian, G. Pan and M. -S. Alouini, "On NOMA-Based mmWave Communications," in *IEEE Transactions on Vehicular Technology*, vol. 69, no. 12, pp. 15398-15411, Dec. 2020.

[5] A. Y. Sadeeq and M. Ahmed, "UAV-BS-based Hybrid OMA-NOMA System with Multiple Antennas for Multi-user Communication," *Journal of Telecommunications and Information Technology*, pp. 38–45, 2025.

[6] L. Zhu, J. Zhang, Z. Xiao, X. -G. Xia and R. Zhang, "Multi-UAV Aided Millimeter-Wave Networks: Positioning, Clustering, and Beamforming," in *IEEE Transactions on Wireless Communications*, vol. 21, no. 7, pp. 4637-4653, July 2022.

[7] Z. Xiao, H. Dong, L. Bai, D. O. Wu and X. -G. Xia, "Unmanned Aerial Vehicle Base Station (UAV-BS) Deployment With Millimeter-Wave Beamforming," in *IEEE Internet of Things Journal*, vol. 7, no. 2, pp. 1336-1349, Feb. 2020.

[8] W. Feng *et al.*, "Joint 3D Trajectory and Power Optimization for UAV-Aided mmWave MIMO-NOMA Networks," in *IEEE Transactions on Communications*, vol. 69, no. 4, pp. 2346-2358, April 2021.

[9] J. Ghosh, V. Sharma, H. Haci, S. Singh and I. -H. Ra, "Performance Investigation of NOMA Versus OMA Techniques for mmWave Massive MIMO Communications," in *IEEE Access*, vol. 9, pp. 125300-125308, 2021.

[10] J. Bao, Z. Cui, Y. Miao, Q. Zhu, K. Mao and B. Hua, "Doppler effects in UAV-to-vehicle multipath channels under 6D mobility," *IET Microwaves, Antennas & Propagation*, vol. 18, no. 12, pp. 1042–1054, 2024.

[11] O. Maraqa, A. S. Rajasekaran, S. Al-Ahmadi, H. Yanikomeroglu and S. M. Sait, "A Survey of Rate-Optimal Power Domain NOMA With Enabling Technologies of Future Wireless Networks," in *IEEE Communications Surveys & Tutorials*, vol. 22, no. 4, pp. 2192-2235, Fourthquarter 2020.

[12] L. M. Mei, M. S. Johal, F. Idris and N. Hashim, "Spectrally efficient UAV communications using non-orthogonal multiple access (NOMA)," *Journal of Advanced Research in AppliedSciencesand Engineering Technology*, vol. 43, no. 1, pp. 227–242. 2025.

[13] M. F. Sohail, C. Y. Leow and S. Won, "Non-Orthogonal Multiple Access for Unmanned Aerial Vehicle Assisted Communication," in *IEEE Access*, vol. 6, pp. 22716-22727, 2018.

[14] W. Feng *et al.*, "Joint 3D Trajectory Design and Time Allocation for UAV-Enabled Wireless Power Transfer Networks," in *IEEE Transactions on Vehicular Technology*, vol. 69, no. 9, pp. 9265-9278, Sept. 2020.

[15] M. Berbineau *et al.*, "Channel Models for Performance Evaluation of Wireless Systems in Railway Environments," in *IEEE Access*, vol. 9, pp. 45903-45918, 2021.

[16] N. T. Nguyen, K. Lee and H. Dai, "Hybrid Beamforming and Adaptive RF Chain Activation for Uplink Cell-Free Millimeter-Wave Massive MIMO Systems," in *IEEE Transactions on Vehicular Technology*, vol. 71, no. 8, pp. 8739-8755, Aug. 2022.

[17] J. Miranda *et al.*, "Path loss exponent analysis in Wireless Sensor Networks: Experimental evaluation," *2013 11th IEEE International Conference on Industrial Informatics (INDIN)*, Bochum, Germany, pp. 54-58, 2013.

[18] M. Jain, S. Soni, N. Sharma and D. Rawal, "Performance analysis at far and near user in NOMA based system in presence of SIC error," *AEU - International Journal of Electronics and Communications*, vol. 114, p. 152993, 2020.

[19] A. A. Saeed and M. A. Ahmed, "Cognitive Radio Based NOMA for The Next Generations of Wireless Communications," *2022 International Conference on Electrical Engineering and Informatics (ICELTICs)*, Banda Aceh, Indonesia, pp. 125-130, 2022.

[20] A. Townsend, I. N. Jiya, C. Martinson, D. Bessarabov and R. Gouws, "A comprehensive review of energy sources for unmanned aerial vehicles, their shortfalls and opportunities for improvements," *Heliyon*, vol. 6, no. 11, p. e05285, 2020.

Ameer Yaseen Sadeeq received his B.Sc. degree in Electronic Engineering – Communication from the University of Mosul, Iraq, in 2017, and his M.Sc. degree in Electronic Engineering – Communication from the University of Ninevah, Iraq, in 2025. He has extensive professional experience in telecommunications and electrical engineering, focusing on network installation, maintenance, and optimization. His research interests include UAV-based mmWave MIMO systems, NOMA/OMA techniques, and power allocation optimization. He possesses strong skills in MATLAB, network configuration, and signal analysis, and completed professional training at Korek Telecom on Huawei equipment maintenance in 2023, along with CCNA and HSE certifications

Mohamad Abdulrahman Ahmed Alhabbar is an Assistant Professor of Digital Communications at the College of Electronics Engineering, Ninevah University, Mosul, Iraq. He received his BSc in Electrical Engineering (Electronics and Communication) from Mosul University in 1999, and his MSc (with distinction) and PhD in Communication and Signal Processing from Newcastle University, UK, in 2009 and 2017, respectively. His research focuses on signal processing for wireless communications, with interests in numerical, simulation, and theoretical performance analysis for next-generation systems. He also works on digital communications, RF and microwave engineering, and digital signal processing. He is an Associate Fellow of the UK Higher Education Academy (AFHEA).